Communication

Tellurium-Doped Bioactive Glassinduces Ferroptosis in Osteosarcoma Cells Regardless of FSP1

Elzbieta Pańczyszyn , Mari Lallukka , Mara Gagliardi , Valentina Saverio , Romina Monzani , Marta Miola , Enrica Verné , Marco Corazzari *

Posted Date: 19 September 2024

doi: 10.20944/preprints202409.1377.v2

Keywords: Ferroptosis; Tellurium; osteosarcoma; FSP1; bioactive glass

Communication

Tellurium-Doped Bioactive Glass Induces Ferroptosis in Osteosarcoma Cells Regardless of FSP1

Elzbieta Pańczyszyn [1], Mari Lallukka [2], Mara Gagliardi [3], Valentina Saverio [1], Romina Monzani [1], Marta Miola [2], Enrica Verné [2] and Marco Corazzari [3,*]

[1] Department of Health Science & Center for Translational Research on Autoimmune and Allergic Disease (CAAD), University of Piemonte Orientale, 28100 Novara, Italy; elzbieta.panczyszyn@uniupo.it; valentina.saverio@uniupo.it; romina.monzani@uniupo.it

[2] Applied Science and Technology Department, Politecnico di Torino, 10129 Torino, Italy; mari.lallukka@polito.it; marta.miola@polito.it; erica.verne@polito.it;

[3] Department of Health Science & Center for Translational Research on Autoimmune and Allergic Disease (CAAD), University of Piemonte Orientale, 28100 Novara, Italy; Interdisciplinary Research Center of Autoimmune Diseases (IRCAD), University of Piemonte Orientale, Novara, Italy; mara.gagliardi@uniupo.it; marco.corazzari@uniupo.it

* Correspondence: marco.corazzari@uniupo.it

Abstract: Human osteosarcoma (OS) is a rare tumor predominantly affecting long bones and characterized by a poor prognosis. Currently, the first line of intervention consists of surgical resection of primary tumors combined with radiotherapy and chemotherapy, with a profound impact on patient's life. Since surgical removal of OS frequently results in large resection of bones the use of biomaterials to sustain the stability of remaining tissue and to stimulate bone regeneration is challenging. Moreover, residual neoplastic cells might be responsible for tumor recurrence. Here we explored the potential of tellurium ion doped bioactive glass as novel therapeutic intervention to both eradicate residual malignant cells and promote bone regeneration. Bioactive glass (BAG) has been extensively studied and employed in the field of regenerative medicine, due to its osseointegration properties and ability to improve bone tissue regeneration. We found that the incorporation of tellurium (Te) in BAG selectively kills OS cells through ferroptosis while preserving the viability of hBMSCs, and stimulating their osteodifferentiation. Although the mechanism of Te toxicity is still unclear: i) Te-BAG generates lipid-ROS through LOXs activity but not iron overload; ii) Te-dependent ferroptosis is mediated by GPX4 down-regulation, and iii) abrogates the anti-ferroptotic activity of FSP1, which expression confers resistance of OS to canonical induction of ferroptosis.

Keywords: ferroptosis; tellurium; osteosarcoma; FSP1; bioactive glass

1. Introduction

The recently described iron-dependent and non-apoptotic form cell death named ferroptosis is under intensive studies as new potential anticancer therapeutic frontier [1]. This is mainly due to the generalized enhanced ferroptosis sensitivity of intrinsic and acquired resistance of cancer cells to apoptosis, the main cell death modality induced by conventional anticancer therapy [2]. Moreover, the still controversial crosstalk with the immune system, which might efficiently contribute for a better tumor eradication, enhances the potential therapeutic impact of ferroptosis in this field of application [3].

Although the modulation of cellular iron metabolism, generated by enhanced iron uptake and/or increased intracellular iron storage mobilization through ferritinophagy, is considered the key step to increase the intracellular labile iron pool (LIP) responsible for lipid peroxides generation, other mechanism, such as the activation of iron-dependent enzymes lipoxygenases (LOX) [4,5] or cytochrome P450 oxidoreductase (POR) [6], are also involved.

 doi:10.20944/preprints202409.1377.v

Independently from the mechanism by which they are generated, lipid peroxides (lipid-ROS) represent the main executioners of this form of cell death, mainly due to their high reactivity and incorporation into cell membranes as phospholipids (mainly PE-OOH), thus compromising the structure and/or membrane functions, resulting in cell death, although the precise molecular mechanisms are still elusive [7].

On the other hand, cells evolved mechanisms to avoid accidental and/or improper induction/execution of ferroptosis, mainly focused on lipid-ROS detoxification, with many cancer cells that use those mechanisms to efficiently escape from ferroptosis execution. In this context, the signaling pathway linking the membrane glutamate/cystine antiporter system (system XC^-) and the glutathione peroxidase 4 (GPX4) represent the main anti-ferroptotic system, through which cystine intake is used to produce GSH that is used by GPX4 to reduce lipid peroxides [1,8]. The latter molecules can also be alternatively destroyed by i) the GCH1-dependent BH4/BH2 cycle or by ii) the FSP1-dependent reduced CoQ1 [9]. Lipid-ROS can also be targeted by iii) members of the aldo-keto reductase superfamily of enzymes (AKRs), thus blocking the execution phase of ferroptosis [5,10], while iv) the ESCRT-III system efficiently repairs the lipid peroxidation-mediated membrane damages, thus conferring resistance to ferroptotic cell death [11]. In addition to the above-mentioned and well-characterized anti-ferroptotic mechanisms, others are emerging with important implications for the ferroptotic-based therapeutic treatment of tumors, such as the one regulated by TG2, although the molecular details are still being studied [12].

Osteosarcoma (OS) is a common malignant bone tumor affecting mainly children, adolescents, and young adults. It arises from osteoid and immature bone, often in the long bones' metaphysis [13]. Despite treatment involving surgery and chemotherapy, OS has a high mortality rate and poor prognosis, with drug resistance being a significant issue [14]. Immune checkpoint inhibitors (ICIs) have shown promise in other cancers but have yet to prove effective in OS [15]. Research to enhance understanding and find new treatment approaches for OS is crucial due to limited progress in improving survival rates. Indeed, we have recently discovered that the sensitivity to ferroptotic cell death by osteosarcoma cells is subordinate to the levels of FSP1, while inhibiting the expression or activity of this factor efficiently re-sensitize cells to ferroptosis [16].

Importantly, surgical removal of primary OS frequently results in large resection of bones, therefore, the use of biomaterials to sustain the stability of remaining tissue and to stimulate bone tissue regeneration is a challenge. Recently, the potential of ion doped bioactive glass as novel therapeutic intervention to both eradicate malignant cells and simultaneously promote bone tissue regeneration is emerging [17]. Bioactive glass (BAG) has been extensively studied and employed in the field of regenerative medicine, due to its osseointegration properties and ability to improve bone tissue regeneration [18]. Of note, we found that the incorporation of tellurium (Te) in BAG resulted in selective OS cells killing through ferroptosis while preserving the viability of human mesenchymal stem cells (hBMSCs), and stimulating their osteodifferentiation. Although the molecular basis of Te toxicity has not yet been fully elucidated, our results suggest that Te-BAG-induces lipid peroxidation, does not require iron overload, and potentially directly affects the functionality of FSP1.

2. Materials and Methods

Cell Culture and Treatments

Human osteosarcoma cell lines – U2OS, MG63 and HOS – were maintained in Dulbecco's modified Eagle's medium (DMEM, EuroClone), supplemented with 10% fetal bovine serum (FBS, EuroClone), 2 mM L-glutamine (Merck), and 1% penicillin/streptomycin (Merck), at 37°C in a humidified incubator with 5% CO2.

Human bone marrow-derived stem cells (hBMSCs) were kindly provided by Prof. P. Genever, University of York. hBMSCs were isolated from the bone marrow and then immortalized using hTERT lentiviral vectors (hBMSCs Y201). Cells were maintained in Dulbecco's modified Eagle's medium (DMEM, EuroClone) supplemented with 15% fetal bovine serum (FBS, EuroClone), 2 mM L-glutamine (Merck), and 1% penicillin/streptomycin (Merck) at 37°C in a humidified incubator with 5% CO_2. Cells were treated with RSL3 (Cayman Chemical) 0.5 μM, Ferrostatin-1 (Merck) 10 μM, AC-

 doi:10.20944/preprints202409.1377.v

DEVD (Cayman Chemical) 10 μM, iFSP1 (BioVision) 6 μM, Deferoxamine (Merck) 10 μM, or Baicalein (Merck) 20 μM, as indicated.

Bioactive Glass Synthesis

Silica-based bioactive glass doped with tellurium dioxide (TeO_2) was developed as previously reported by Miola et al. [19] Two glass compositions (STe0 and STe5), as reported in Table 1, were developed by partially substituting SiO_2 with TeO_2. The amount of TeO_2 was selected considering a potential toxic effect of this element, as previously described [19–22]. Briefly, the glasses were synthesized by melting the reactants in a Pt crucible at 1450 °C, pouring the melt in a brass mol and annealing them at 550 °C for 14 h. The obtained bars were cut in disc-shaped specimens (10 x 2mm) and polished with abrasive SiC papers [19]. Biological characterization was performed on the discs. Specimens were heat-sterilized for 3h at 180°C and stored at room temperature prior to biological experiments.

Table 1. Nominal compositions of the investigated glasses.

	% mol	
	STe0	STe5
SiO_2	48.6	43.6
Na_2O	16.7	16.7
CaO	34.2	34.2
P_2O_5	0.5	0.5
TeO_2	0.0	5.0

Cytocompatibility Evaluation

The cytocompatibility of the investigated bioactive glass was tested in an indirect exposure culture, as previously described [23]. Briefly, specimens of STe0 and STe5 were soaked in 1.5 ml of culture medium for 72h at 37°C, to stimulate iron release [23]. Subsequently, osteosarcoma cells and hBMSCs were exposed to STe0/STe5 conditioned medium for 72h.

Cell Viability

Cell viability was measured using the AlamarBlue™ reagent (Bio-Rad) according to the manufacturer's instructions, as previously described [24]. Briefly, 15 x 10^3 cells/well were plated in 24-wellplates, treated as indicated. The cell medium was discarded and an appropriate amount of AlamarBlue reagent was added. Cells were incubated for 4h, and fluorescence was monitored (530-560 nm excitation and 590 nm emission wavelengths) using a TECAN automation platform.

Fluorescein diacetate (FDA)/7AAD staining was used to identify and measure the percentage of live/dead cells [12]. Briefly, cells were incubated (15-20 min) with PBS containing FDA (7 pg/ml; Thermo Fisher Scientific) and 7AAD (50 ng/ml; Bio-Rad) and 10.000 events were acquired using flow cytometry (FACSymphony, BD). The percentage of 7AAD positive and FDA negative cells was measured and is indicated as 'cell death (%)'.

Real Time PCR (qPCR)

Total RNA was isolated using TripleXtractor reagent (Grisp), and ExcelRT Reverse Transcriptase (Grisp) was used to produce cDNA using 2 μg of total RNA. Quantitative PCR (qPCR) reactions were performed using the Excel-Taq FAST qPCR SybrGreen (Grisp) and a CFX96 thermocycler (Bio-Rad). Primer sequences were designed using the online IDT PrimerQuest Tool software (IDT; https://eu.idtdna.com/Primerquest/Home/Index) and sequences are reported below [25].

Name	Sequence

 doi:10.20944/preprints202409.1377.v

AKR1C1	GCCGTGGAGAAGTGTAAAG/CAGACAGGCTTGTACTTGAG
ALP	GAGTATGAGAGTGACGAGAAAG/GAAGTGGGAGTGCTTGTATC
BSP	CAGAAGAGGAGGAGGAAGAA/CCCAGTGTTGTAGCAGAAAG
COL1	GGATTCCAGTTCGAGTATGG/CAGTGGTAGGTGATGTTCTG
DMT1	GCTGTCTTCCAAGATGTAGAG/GGATGGGTATGAGAGCAAAG
FSP1	CCTGCCCTTCTCTCATCTTA/GTCCTCATAGGCCTGGATAG
GPX4	AGCTCTTCTGGGAAGTAGAC/CCTCCCTGTACCACATCTAT
L34	GTCCCCGAACCCTGGTAATAGA/GGCCCTGCTGACATGTTTCTT
NQO1	GGATGAGACACCACTGTATTT/CTCCTCATCCTGTACCTCTT
NRF2	CCTGCCCTTCTCTCATCTTA/GTCCTCATAGGCCTGGATAG
OPN	CCCATCTCAGAAGCAGAATC/TGGCTTTCGTTGGACTTAC
PTGS2	GCCTGGTCTGATGATGTATG/GTATTAGCCTGCTTGTCTGG
RUNX2	GAATGCCTCTGCTGTTATGA/GAAGACGGTTATGGTCAAGG
SLC7A11	CTGGGTTTCTTGTCCCATATAA/GTTGCCCTTTCCCTCTATTC
TfR1	GTGAGGGATCTGAACCAATAC/TGGAAGTAGCACGGAAGA

The L34 mRNA level was used as an internal control and the comparative Ct method (ΔΔCt) was used for relative quantification of gene expression.

Western Blotting Analysis

Proteins were isolated by using a RIPA Buffer supplemented with a protease inhibitor cocktail (Merck), and an equal amount of proteins (20 µg) were subjected to an SDS-PAGE, and electroblotted onto nitrocellulose membranes (Bio-Rad). Membranes were blocked for 1h with 5% non-fat dry milk (Merck) in PBS plus 0.1% Tween20 (Merck) and incubated with the indicated primary antibodies in blocking solution overnight at 4°C: anti-FSP1 (1:1000, ProteinTech), anti-NRF2 (1:1000, Cell Signaling Technology), anti-FTH1 (1:1000, Santa Cruz Biotechnology), anti-NCOA4 (ARA70; 1:1000, Santa Cruz Biotechnology), anti-GPX4 (1:1000, Cell Signaling Technology), anti-Tubulin (1:500, Santa Cruz Biotechnology), and anti-GAPDH (1:500, Santa Cruz Biotechnology). Detection was achieved using horseradish peroxidase (HRP)-conjugated secondary antibodies (1:5000; Jackson ImmunoResearch) and visualized using SuperSignal West Pico Plus (Thermo Fisher Scientific). Images were acquired using a ChemiDoc Touch Imaging System (Bio-Rad) and analyzed using Image Lab software (Bio-Rad) [26]. Quantification (densitometric analysis) was performed by using Image Lab software.

Detection of Intracellular Fe^{2+}

A BioTracker FerrOrange Live Cell Dye (Sigma-Aldrich) was used to detect intracellular labile ferrous (Fe2+) ions, according to the manufacturer's protocol, as previously described [16]. Briefly, 15 × 10^3 cells/well U2OS were plated in 24-wellplates and then exposed to STe5 or STe0 for 48h. The cells were then washed twice with PBS and treated with 1 uM FerrOrange in DMEM without FBS for 30 min at 37°C. After incubation, FerrOrange was removed by washing cells twice with PBS, and

 doi:10.20944/preprints202409.1377.v

fluorescent signal was recorded using a THUNDER 3D Cell Imager (Leica). Quantification was performed by using ImageJ software.

Immunofluorescence

Samples were washed with cold PBS and fixed in PFA (Merck) 4% for 15 min at 4°C, permeabilized with 0.5% Triton X-100 (Merck) in cold PBS for 10 min at 4°C, washed twice and incubated with 10% donkey serum (Jackson ImmunoResearch) plus 0.05% Triton X-100 in cold PBS, 30 min at 4°C. Next, the slides were washed and incubated with anti-FSP1 (1:300, ProteinTech) primary antibody in 1% donkey serum plus 0.05% Triton X-100 in cold PBS, 1 h at 4°C. After washing, the slides were incubated with appropriate secondary antibodies (Jackson ImmunoResearch) 1:500 in 1% donkey serum plus 0.05% Triton X-100 in cold PBS and incubated for 1 h at 4 °C.

Coverslips were mounted onto glass using ProLong Gold Antifade with DAPI mounting solution (Thermo Fisher Scientific). Images were acquired using an SP8 confocal microscope (Leica)[25].

Statistical Analysis

The experiments were performed in triplicate and repeated at least three times. Statistical analyses were performed using the GraphPad software (GraphPad Software; GraphPad Prism 6). Student's t-test or ANOVA was used to determine the statistical significance. A p-value of equal to or less than 0.05 was considered significant. mRNA expression levels are represented as 'fold change,' relative levels. Histograms represent mean ± SD; **** $p < 0.0001$; *** $p < 0.001$; ** $p < 0.01$; * $p < 0.05$; ns non-significant.

3. Results

3.1. Selective Toxicity of Tellurium-Doped Bioactive Glass to Osteosarcoma Cells and Osteoinductive Effect on hBMSCs

The biomaterial-based strategy represents an innovative solution that is capable of simultaneously providing tumor therapy and promoting bone regeneration [27]. Bioactive glasses (BAGs), which possess the distinctive capacity to adhere to both hard and soft tissues and are primarily used for bone regeneration purposes, are currently undergoing extensive investigation, and are tailored towards the development of drug delivery systems, as well as antibiotic, hemostatic, and cancer-killing therapies [28]. In this sense, the incorporation of inorganic ions, such as silver (Ag^{+}), copper (Cu^{2+}), and zinc (Zn^{2+}), into the structure of BAGs endows them with specific biological functions and thus improves their effectiveness [18]. Therefore, we investigated the osteoinductive and anticancer properties of silica-based bioactive glass containing a low amount of tellurium dioxide (TeO_2) as this active element and its compounds are currently being discovered as novel and valid cancer therapeutics [29]. To this end, and to confirm our previous results on cytocompatibility [19], we treated our panel of human osteosarcoma cells (U2OS, MG63, and HOS) and human bone marrow stem cells (hBMSC) with a medium conditioned with dissolution products of tellurium-doped BAG (STe5) or base BAG composition (STe0), and cell viability was measured after 72h. Data reported in *Figure 1*A indicate that the addition of tellurium to BAG efficiently killed osteosarcoma cells, increasing the number of dead cells to 25% for U2OS, 36% for HOS, and 24% for MG63, while no significant deleterious effect was observed on hBMSCs. Thus, these results suggest the potential selective toxicity of Te-doped bioactive glass (Te-BAG) to bone cancer cells.

Since the first report of its bone-binding properties nearly 40 years ago, the bioactive glass (45S5, Bioglass®) has been extensively investigated for biomedical applications. A significant characteristic of this material is its bioactivity, leading to release of functional ions such as Ca^{2+} and PO_4^{3-} when in contact with biological fluids. This facilitates the creation of a layer of nanocrystalline hydroxyapatite (HA) on the glass surface, which has a strong affinity for living tissue. Moreover, such ionic dissolution products are well-known to effectively promote differentiation into bone-forming cells and mineralization of the extracellular matrix [30]. Therefore, we evaluated the levels of osteogenic

 doi:10.20944/preprints202409.1377.v

differentiation markers, such as RUNX2, ALP, COL1, OPN, and BSP171, in hBMSC exposed to media conditioned with ionic dissolution products of STe0 and STe5. Interestingly, enhanced mRNA expression of the indicated osteogenesis markers was evident after 72h of culture with extracts derived from tellurium-doped bioactive glass (STe5). In contrast, samples without tellurium(STe0) exhibited lower osteostimulation effects on hBMSC (*Figure 1*B-C). Of note, RUNX2 and ALP are consistently referred to as early transcription factors and are predominantly expressed in preosteoblasts and osteoblasts [31]. Collectively, our results indicated that the expression of genes specific to osteoblasts was significantly enhanced by the medium conditioned by STe5, thus suggesting the potential use of Te-BAG as a platform for bone regeneration and targeted therapy for osteosarcoma.

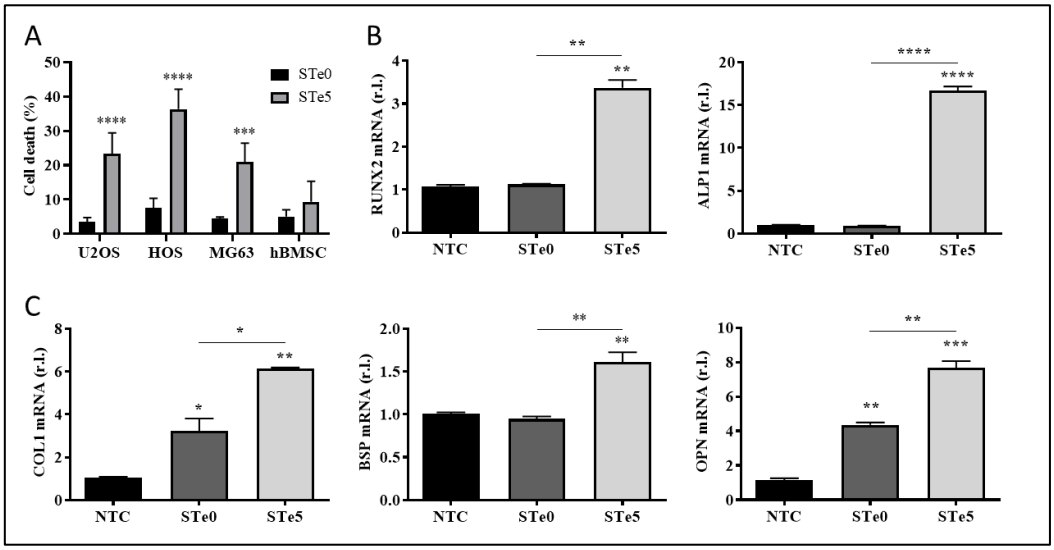

Figure 1. STe5 kills OS cells while inducing osteogenic markers in hBMSCs. (A) The indicate OS cell lines and hBMSCs were exposed to balk BAGs- (STe0) or tellurium doped BAGs- (STe5) conditioned media and cell death was evaluated after 72h. (B) hBMSC were exposed to STe0- or STe5-conditioned media and the expression of the indicated pro-osteogenic markers was evaluated by qPCR, after 72h. Experiments were performed in triplicate and repeated three times. Histograms represent the mean ± SD; * p <0.05; ** p <0.01; *** p <0.001; **** p <0.0001.

3.2. Tellurium-Doped Bioactive Glass Induces Ferroptosis-Mediated OS Cells Death

Apoptosis has long been considered a deliberate mechanism of regulated cell death (RCD) and the pathways involved in this process have been extensively studied in various types of tumor cells. The induction of apoptosis is recognized as a prominent therapeutic approach for eliminating cancer cells *[32,33]*. However, accumulating evidence have proven that anti-tumor strategies based on the induction of the non-apoptotic form of RCD known as ferroptosis is a promising direction for addressing certain challenges in cancer therapy *[5,10,32]*. Therefore, to identify the process underlying the observed toxicity of tellurium-doped bioactive glass to OS cells, we evaluated the involvement of both apoptosis and ferroptosis. To this end, the three OS cell lines were exposed to STe5 in the presence or absence of the ferroptosis inhibitor ferrostatin-1 (Fer1) or the apoptosis inhibitor AC-DEVD [34] for 72h, while STe0 was used as a control. Data reported in *Figure 2*A clearly show that the cytotoxic effect by STe5 was consistently inhibited by ferrostatin-1 (STe5+Fer1), while AC-DEVD was ineffective.

Subsequently, the evaluation of the ferroptotic markers PTGS2, ACSL4, and CHAC1 supported the induction of this form of cell death in cells exposed (48h) to medium conditioned with STe5 compared to samples without tellurium (STe0; *Figure 2*B). Additionally, ferroptotic cell death induced by STe5 was further confirmed in HOS cells by the typical morphological features characterized by plasma membrane bubbling (*Figure 2*C) [35]. Importantly, Te-dependent morphological change was

 doi:10.20944/preprints202409.1377.v

completely prevented by the concomitant exposure to Fer1, while AC-DEVD was ineffective (*Figure* 2C).

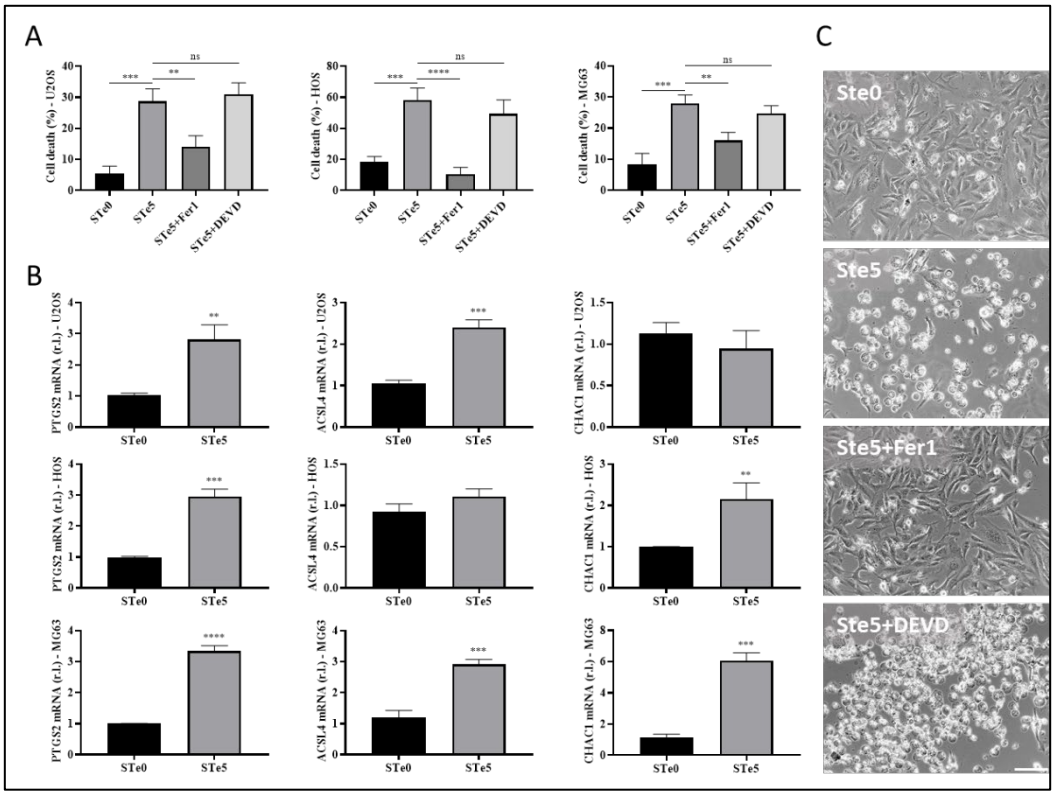

Figure 2. Tellurium-doped BAG specifically induces ferroptosis in OS cells. (A) The indicated OS cell lines (U2OS, MG63 and HOS) were exposed to conditioned medium by STe5 alone or in presence of the ferroptosis inhibitor Fer1 (10 μM) or the apoptosis inhibitor AC-DEVD (10 μM), and cell viability was evaluated after 48h. STe0-conditioned medium was used as a control. (B) U2OS (upper panels), HOS (middle panels) or MG63 (bottom panels) were exposed to STe0- or STe5- conditioned media and the expression of the pro-ferroptotic markers PTGS2, ACSL4 or CHAC1 was evaluated by qPCR, after 72 h. (C) HOS were exposed to conditioned medium by STe0 or STe5 alone or in the presence of Fer1 (10 μM) or AC-DEVD (10 μM), and cell morphology was evaluated by light microscopy (phase contrast), at 72h. The appearance of cell membrane blebbing, characteristic of cells dying through ferroptosis, is evidenced by green arrows (scale bar 100 μm). Experiments were performed in triplicate and repeated three times. Histograms represent the mean ± SD; ** p <0.01; *** p <0.001; **** p <0.0001.

Hence, our results confirmed the anticancer properties of tellurium-doped bioactive glass, indicating that ferroptosis is the main pathway of RCD responsible for its cytotoxic effect on osteosarcoma cells.

Of note, Te-BAG efficiently induced ferroptosis also in U2OS cells, a cell line that we recently identified as the most resistant to the conventional induction and execution of ferroptotic cell death, compared to both MG63 and HOS, due to the enhanced expression of FSP1 [16]. Thus, U2OS cells were used for further investigations aimed at identifying potential molecular targets and/or cellular mechanisms underlying the cancer cell-specific toxic effect of Te-BAG, which is capable of re-sensitizing OS cells to ferroptosis.

3.3. Role of Iron in Te-BAG-Induced Ferroptosis

Recently, Liu and co-workers reported that macrophages exposed to tellurium compounds exhibited ferroptosis, the induction of which was associated with the degradation of ferritin heavy chain 1 (FTH1), the primary protein responsible for intracellular iron storage, through an autophagy-

 doi:10.20944/preprints202409.1377.v

based process known as ferritinophagy [36]. The occurrence of intracellular iron overload, a hallmark of ferroptosis, resulting from this process subsequently promotes the production of lipid peroxides [37]. To investigate whether Te-BAG triggers ferroptosis in OS cells by disrupting intracellular iron homeostasis, U2OS cells were exposed to medium conditioned with STe5 in the presence of the iron chelator and ferroptosis inhibitor deferoxamine (DFO). Remarkably, DFO significantly decreased the cytotoxic effect of STe5, as shown in *Figure 3*A, indicating a potential involvement of iron in the STe5-stimulated lipid peroxidation.

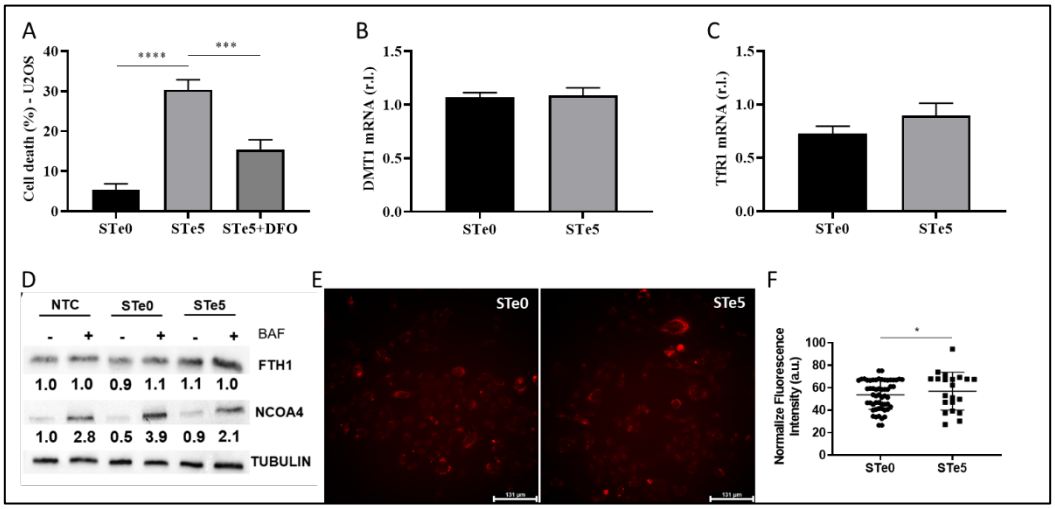

Figure 3. Te-BAGs-induced ferroptosis does not affect iron metabolism. (A) U2OS cells were exposed to conditioned medium by STe5 alone or in combination with iron chelator deferoxamine (DFO, 10 μM), and cell viability was evaluated at 72h. STe0-conditioned medium was used as a control. The expression of divalent metal transporter 1 (DMT1; B) or transferrin receptor 1 (TfR1; C) was evaluated in cells treated as in A, at 48h. (C) The expression of the ferritinophagy markers ferritin heavy chain 1 (FTH1) and nuclear receptor coactivator 4 (NCOA4) was evaluated in U2OS cells exposed to STe5- or STe0-conditioned medium, alone or in combination with autophagy inhibitor bafilomycin A1 (BAF), by western blotting. Tubulin was used as a loading control, and results of densitometric analysis were reported for each corresponding band. (E) U2OS cells were exposed to tellurium-doped bioactive glass- (STe5) or basal composition- (STe0) conditioned medium for 48h and the intracellular Fe^{2+} was evaluated by confocal microscopy (in red), using FerrOrange probe. Scale bar = 131μm. FerroOrange fluorescence quantification was performed by using ImageJ (F). Experiments were performed in triplicate and repeated three times. Histograms represent the mean ± SD; *** p <0.001; **** p <0.0001.

To gain deeper insight into the involvement of iron-dependent pathways in Te-BAG-induced ferroptosis, we also evaluated the expression profiles of key signaling molecules involved in iron uptake and transport, such as TfR1 and DMT1 [16]. However, any notable alteration in the expression of these signaling molecules was observed upon exposure of U2OS cells to STe5-conditioned medium, when compared to samples derived from basal BAG composition (STe0; *Figure 3*B-C). Next, we explored the potential of Te-BAG to induce ferroptosis through the activation of ferritinophagy, a type of autophagy relaying on NCOA4-mediated and lysosome-dependent degradation of ferritin-iron aggregates. Regardless, our finding showed no significant alterations in NCOA4 or FTH1 protein levels that would suggest the activation of this process, in cells exposed to STe5 compared to STe0, when autophagy was inhibited by bafilomycin A1 (BAF; *Figure 3*D). Therefore, our data indicate that although iron seems to be involved in the execution of ferroptosis of OS cells exposed to Tellurium, no evident alteration of Fe metabolism was observed. This conclusion is further sustained by measuring the intracellular iron concentration by staining cells with FerrOrange. Indeed, although intracellular iron accumulation is frequently observed in cells dying through ferroptosis, our analysis revealed no increase in free iron content in U2OS cells exposed to STe5 (*Figure 3*E). Collectively, our

 doi:10.20944/preprints202409.1377.v

findings suggest that the mechanism underlying Te-BAG-induced ferroptosis does not involve the disruption of cellular iron uptake and storage or intracellular iron overload.

3.4. Te-BAG-Induced Ferroptosis Circumvents the Inhibitory Activity of FSP1

Although the molecular basis of Te toxicity has not yet been fully determined, one of the potential mechanisms is the substitution of the sulfur group in various amino acids, leading to the formation of dysfunctional proteins. Moreover, based on the homologies observed in the characteristics of elements belonging to the same group as tellurium, such as selenium, another hypothesis on the potential mechanism of cytotoxicity depends on its ability to oxidize glutathione (GSH), which causes the accumulation of ROS [38] and, possibly, lipid peroxides. Indeed, Wu and colleagues recently reported the introduction of Te nanowires as an inorganic prodrug with the capability to selectively deplete glutathione and elevate ROS levels to lethal thresholds in cancer cells without inducing oxidative stress in normal cells [39]. Moreover, the disruption of redox homeostasis observed in the presence of Te compounds was also correlated with a decrease in NRF2 level [36]. Thus, we examined the expression of two key antioxidant factors, GPX4 and NRF2. Of note, ROS production/accumulation and dysregulation of NRF2 and GPX4 expression/activity are also biomarkers of ferroptosis, with GPX4 directly involved in lipid-ROS demolition. Indeed, we observed decreased GPX4 expression in U2OS cells exposed to STe5-conditioned medium, while no significant changes in NRF2 and direct target NQO1 expression were noted, in the same experimental conditions, compared to cells exposed to STe0-conditioned medium (*Figure 4*A-C).

We also found increased expression of SLC7A11 in cells exposed to Tellurium, as the cells try to counteract the reduced GPX4 activity by increasing GSH production (*Figure 4*D).

Importantly, cytotoxic effect of STe5 was effectively abolished by concomitant exposure of cells (U2OS) to STe5 and baicalein (BAI; *Figure 4*E), which inhibits Lipoxygenases (LOXs) activity *[10,40,41]*. These data confirm the key role played by lipid-ROS in Te-BAG-induced ferroptosis.

Next, we examined the role of FSP1 in the ferroptotic process elicited by tellurium-doped bioglass. Specifically, we analyzed the reason why this critical antioxidant pathway, which contributes to the cellular resistance of U2OS cells under conventional ferroptosis induction [16], is insufficient to protect against the process triggered by Te. In fact, as reported in *Figure 4*F, simultaneous administration of STe5 and iFSP1, which specifically inhibits FSP1 activity, did not result in a significant increase in cell sensitivity to ferroptosis execution (*Figure 4*F). Notably, the effect of iFSP1, which sensitizes cells to ferroptotic cell death, was observed in cells exposed to basic materials (STe0), implying that tellurium may interfere with FSP1 activity. Finally, while FSP1 expression was enhanced in U2OS cells exposed to RLS3, as expected [16], no significant changes were observed in cells exposed to STe5-conditioned medium, compared to STe0-conditioned medium (*Figure 4*G).

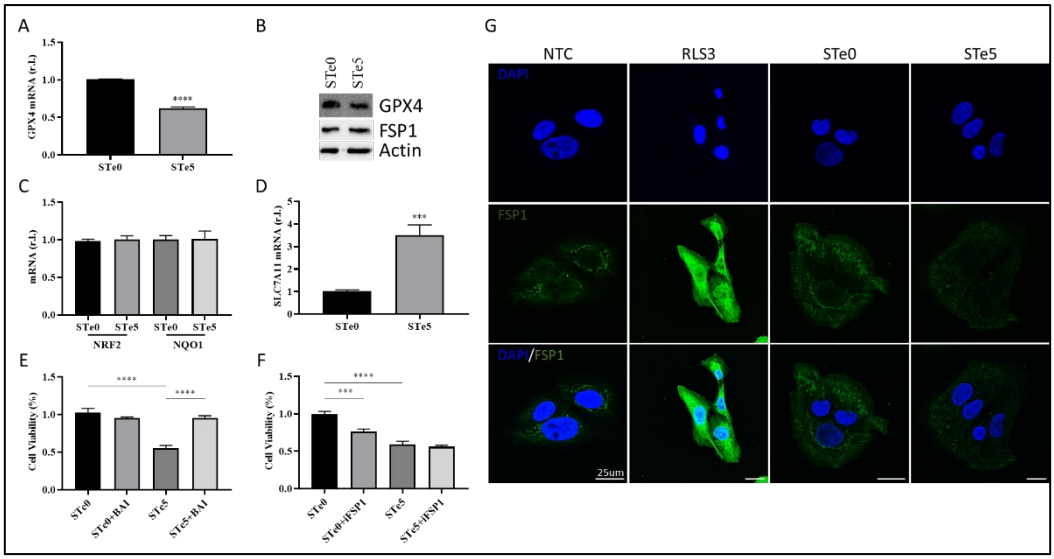

 doi:10.20944/preprints202409.1377.v

Figure 4. Te-BAG-induces ferroptosis regardless to FSP1 but ignited by GPX4 down-regulation. U2OS were exposed to STe5- or STe0- conditioned medium (48h) an the levels of GPX4 mRNA (A) or protein (B) were evaluated together with the mRNA levels of NRF2, NQO1 (C), or SLC7A11 (D), by qPCR or western blotting analysis (Actin was used as loading control). Cells were exposed to medium conditioned by STe0 or STe5 alone or in the presence of Baicalein (BAI, 10 μM; E) or FSP1 inhibitor (iFSP1, 10 μM; F), and cell viability was evaluated at 72h. Finally, U2OS were exposed or unexposed to RLS3 (0.5 μM) or to STe0- or STe5- conditioned medium and FSP1 expression was evaluated by immunofluorescence (G). FSP1 was evidenced by anti-FSP1 antibody (green) while nuclei were stained with DAPI (blue). Scale bar 25 μm. Experiments were performed in triplicate and repeated three times. Histograms represent the mean ± SD; *** p <0.001; **** p <0.0001.

4. Discussion

Osteosarcoma is a rare disease affecting bone tissues with primary treatment represented by extensive surgical resection coupled to chemotherapy, radiotherapy, and immunotherapy, using drugs like methotrexate, cisplatin, doxorubicin, and ifosfamide [42,43]. Despite advances, 5-year survival rates remain around 70%, with challenges including side effects from high-dose chemotherapy and drug resistance [44]. Targeted therapy, focusing on specific molecular and cellular pathways, is emerging as a promising approach [14,45,46], and immune checkpoint inhibitors, like mifamurtide, show potential in improving survival [47,48].

However, complete eradication of cancer cells is obviously very difficult even when large portions of surrounding tissues are included in the resection. Of note, surgical resection comes with very invalidating conditions experienced by patients, which are frequently very young. Furthermore, tumor recurrence is a non-negligible factor, potentially due to undetectable residual cancer cells [49,50]. Therefore, new therapeutic strategies are urgently needed to effectively remove the neoplasm and minimize the impact on the affected bones.

In this context, the development of new biomaterial formulations joining together both osteogenic properties, to stimulate tissue regeneration, and anticancer activity, to eradicate residual neoplastic cells, can represent a formidable innovative treatment for these patients. Indeed, bioactive glass doped with inorganic ions is offering new potential therapeutic opportunities, with the presence of those elements not only increases the known osteogenic properties of bioglass but also confers new biological functions [17]. This is the case of Te-BAGs. Indeed, we found that while this tellurium doped BAG is well tolerated by hBMSCs, Te consistently enhances the pro-osteogenic properties of BAG, at least *in vitro*. Therefore, this biomaterial would accelerate the regeneration of bone tissues, thus improving the healing process. On the other hand, we found that the presence of Te confers a pro-ferroptotic activity to doped BAG. Indeed, tellurium efficiently induced ferroptosis in osteosarcoma cell lines, regardless of the levels of the anti-ferroptotic factor FSP1 we recently described representing a valid biomarker of resistance [16]. Indeed, Te activity seems to rely on two levels: i) to prevent FSP1 upregulation which is observed in cells exposed to canonical pro-ferroptotic drugs (e.g., RLS3), and ii) interfere with its anti-ferroptotic activity.

Although further studies are required to fully elucidate the molecular mechanism by which Te abrogates the anti-ferroptotic properties of FSP1, its pro-ferroptotic activity seems to relay on the downregulation of the main anti-ferroptotic factor GPX4, while increasing the expression of the upstream factor SLC7A11. The latter phenomenon is not surprising since cancer cells respond to reduced expression/activity of GPX4 increasing the uptake of cystine to enhance the production of GSH to be used by GPX4 to reduce lipid-ROS, thus counteracting ferroptosis execution. Moreover, although Te does not dysregulate iron metabolism which typically increases LIP, a hallmark of ferroptosis and responsible for lipid peroxides generation, iron trapping abrogates Te-stimulated ferroptosis. The latter together with the inhibition of ferroptosis stimulated by tellurium by concomitant exposure to baicalein, strongly indicates the involvement of LOXs. Indeed, these are iron-dependent enzymes actively producing PUFA-OOH, thus participating to ferroptosis, which activity can be inhibited by baicalein and/or chelating intracellular iron [5,10].

 doi:10.20944/preprints202409.1377.v

Therefore, it would be interesting to evaluate whether the ability of tellurium to compromise the anti-ferroptotic activity of FSP1 is strictly related to osteosarcoma or is a general feature of this transition element, which would have important implication in cancer therapy.

In conclusion, our work clearly show that Te-BAGs might represent a new valuable opportunity in the clinical management of osteosarcoma due to the combined pro-osteogenic and pro-ferroptotic activities.

Author Contributions: "Conceptualization, M.C., X.X. and Y.Y.; methodology, E.P., M.L., M.G., V.S., R.M.; formal analysis, M.C., E.P.; investigation, E.P., M.L.; writing—original draft preparation, E.P., M.C.; writing—review and editing, M.C., M.M., M.L., and E.V.; supervision, M.C., M.M. and E.V.; project administration, M.C.; funding acquisition, M.C. All authors have read and agreed to the published version of the manuscript."

Funding: This work was supported by the Italian Ministry of Education, University and Research (MUR) program "Departments of Excellence 2018–2022", FOHN Project—Department of Health Sciences, Università del Piemonte Orientale, and MUR Progetti di Ricerca di Rilevante Interesse Nazionale (PRIN) Bando 2022 – grant 202285XS52, FAR 2019 (Progetti di Ateneo), the EU grant "PREMUROSA" (ID #860462), "ExcellMater" (ID #952033) H2020 projects are also acknowledged.

Data Availability Statement: Data generated are reported in the article.

Conflicts of Interest: "The authors declare no conflicts of interest."

References

1. Dixon, S.J., et al., *Ferroptosis: an iron-dependent form of nonapoptotic cell death.* Cell, 2012. **149**(5): p. 1060-72.
2. Zhou, Q., et al., *Ferroptosis in cancer: From molecular mechanisms to therapeutic strategies.* Signal Transduct Target Ther, 2024. **9**(1): p. 55.
3. Zheng, Y., et al., *The crosstalk between ferroptosis and anti-tumor immunity in the tumor microenvironment: molecular mechanisms and therapeutic controversy.* Cancer Commun (Lond), 2023. **43**(10): p. 1071-1096.
4. Corazzari, M. and L. Collavin, *Wild-type and mutant p53 in cancer-related ferroptosis. A matter of stress management?* Front Genet, 2023. **14**: p. 1148192.
5. Gagliardi, M., et al., *Ferroptosis: a new unexpected chance to treat metastatic melanoma?* Cell Cycle, 2020. **19**(19): p. 2411-2425.
6. Zou, Y., et al., *Cytochrome P450 oxidoreductase contributes to phospholipid peroxidation in ferroptosis.* Nat Chem Biol, 2020. **16**(3): p. 302-309.
7. Kagan, V.E., et al., *Oxidized arachidonic and adrenic PEs navigate cells to ferroptosis.* Nat Chem Biol, 2017. **13**(1): p. 81-90.
8. Ingold, I., et al., *Selenium Utilization by GPX4 Is Required to Prevent Hydroperoxide-Induced Ferroptosis.* Cell, 2018. **172**(3): p. 409-422 e21.
9. Doll, S., et al., *FSP1 is a glutathione-independent ferroptosis suppressor.* Nature, 2019. **575**(7784): p. 693-698.
10. Gagliardi, M., et al., *Aldo-keto reductases protect metastatic melanoma from ER stress-independent ferroptosis.* Cell Death Dis, 2019. **10**(12): p. 902.
11. Dai, E., et al., *ESCRT-III-dependent membrane repair blocks ferroptosis.* Biochem Biophys Res Commun, 2020. **522**(2): p. 415-421.
12. Gagliardi, M., et al., *Transglutaminase 2 and Ferroptosis: a new liaison?* Cell Death Discov, 2023. **9**(1): p. 88.
13. Simpson, E. and H.L. Brown, *Understanding osteosarcomas.* JAAPA, 2018. **31**(8): p. 15-19.
14. Li, S., et al., *Targeted therapy for osteosarcoma: a review.* J Cancer Res Clin Oncol, 2023. **149**(9): p. 6785-6797.
15. Zhang, Z., et al., *Immune checkpoint inhibitors in osteosarcoma: A hopeful and challenging future.* Front Pharmacol, 2022. **13**: p. 1031527.
16. Panczyszyn, E., et al., *FSP1 is a predictive biomarker of osteosarcoma cells' susceptibility to ferroptotic cell death and a potential therapeutic target.* Cell Death Discov, 2024. **10**(1): p. 87.
17. Ali, S., I. Farooq, and K. Iqbal, *A review of the effect of various ions on the properties and the clinical applications of novel bioactive glasses in medicine and dentistry.* Saudi Dent J, 2014. **26**(1): p. 1-5.
18. Souza, L., et al., *Cancer Inhibition and* In Vivo *Osteointegration and Compatibility of Gallium-Doped Bioactive Glasses for Osteosarcoma Applications.* ACS Appl Mater Interfaces, 2022. **14**(40): p. 45156-45166.
19. Miola, M., et al., *Tellurium: A new active element for innovative multifunctional bioactive glasses.* Mater Sci Eng C Mater Biol Appl, 2021. **123**: p. 111957.
20. Miola, M. and E. Verne, *Bioactive and Antibacterial Glass Powders Doped with Copper by Ion-Exchange in Aqueous Solutions.* Materials (Basel), 2016. **9**(6).
21. Miola, M., et al., In vitro *study of manganese-doped bioactive glasses for bone regeneration.* Mater Sci Eng C Mater Biol Appl, 2014. **38**: p. 107-18.

22. Verne, E., et al., *Surface characterization of silver-doped bioactive glass.* Biomaterials, 2005. **26**(25): p. 5111-9.
23. Zhong, C.L., et al., *Antioxidant and Antimicrobial Activity of Tellurium Dioxide Nanoparticles Sols.* Journal of Nano Research, 2013. **25**: p. 8-15.
24. Kovrlija, I., et al., *Doxorubicin loaded octacalcium phosphate particles as controlled release drug delivery systems: Physico-chemical characterization,* in vitro *drug release and evaluation of cell death pathway.* Int J Pharm, 2024. **653**: p. 123932.
25. Monzani, R., et al., *The Gut-Ex-Vivo System (GEVS) Is a Dynamic and Versatile Tool for the Study of DNBS-Induced IBD in BALB/C and C57BL/6 Mice, Highlighting the Protective Role of Probiotics.* Biology (Basel), 2022. **11**(11).
26. Pagliarini, V., et al., *Downregulation of E2F1 during ER stress is required to induce apoptosis.* J Cell Sci, 2015. **128**(6): p. 1166-79.
27. Zhang, Y., et al., *Biomaterial-based strategy for bone tumor therapy and bone defect regeneration: An innovative application option.* Frontiers in Materials, 2022. **9**.
28. Kaou, M.H., et al., *Advanced Bioactive Glasses: The Newest Achievements and Breakthroughs in the Area.* Nanomaterials (Basel), 2023. **13**(16).
29. Sandoval, J.M., et al., *Tellurite-induced oxidative stress leads to cell death of murine hepatocarcinoma cells.* Biometals, 2010. **23**(4): p. 623-32.
30. Rahaman, M.N., et al., *Bioactive glass in tissue engineering.* Acta Biomater, 2011. **7**(6): p. 2355-73.
31. Baniwal, S.K., et al., *Runx2 promotes both osteoblastogenesis and novel osteoclastogenic signals in ST2 mesenchymal progenitor cells.* Osteoporos Int, 2012. **23**(4): p. 1399-413.
32. Wang, X., et al., *Non-apoptotic cell death-based cancer therapy: Molecular mechanism, pharmacological modulators, and nanomedicine.* Acta Pharm Sin B, 2022. **12**(9): p. 3567-3593.
33. Ji, P., et al., *Doxorubicin Inhibits Proliferation of Osteosarcoma Cells Through Upregulation of the Notch Signaling Pathway.* Oncol Res, 2014. **22**(4): p. 185-191.
34. Solania, A., G.E. Gonzalez-Paez, and D.W. Wolan, *Selective and Rapid Cell-Permeable Inhibitor of Human Caspase-3.* ACS Chem Biol, 2019. **14**(11): p. 2463-2470.
35. Dodson, M., R. Castro-Portuguez, and D.D. Zhang, *NRF2 plays a critical role in mitigating lipid peroxidation and ferroptosis.* Redox Biol, 2019. **23**: p. 101107.
36. Hassannia, B., P. Vandenabeele, and T. Vanden Berghe, *Targeting Ferroptosis to Iron Out Cancer.* Cancer Cell, 2019. **35**(6): p. 830-849.
37. Fang, X., et al., *The molecular and metabolic landscape of iron and ferroptosis in cardiovascular disease.* Nat Rev Cardiol, 2023. **20**(1): p. 7-23.
38. Cao, W., L. Wang, and H.P. Xu, *Selenium/tellurium containing polymer materials in nanobiotechnology.* Nano Today, 2015. **10**(6): p. 717-736.
39. Wu, Y., et al., *An inorganic prodrug, tellurium nanowires with enhanced ROS generation and GSH depletion for selective cancer therapy.* Chem Sci, 2019. **10**(29): p. 7068-7075.
40. Xie, Y.C., et al., *Identification of baicalein as a ferroptosis inhibitor by natural product library screening.* Biochemical and Biophysical Research Communications, 2016. **473**(4): p. 775-780.
41. Lovat, P.E., et al., *Gangliosides link the acidic sphingomyelinase-mediated induction of ceramide to 12-lipoxygenase-dependent apoptosis of neuroblastoma in response to fenretinide.* J Natl Cancer Inst, 2004. **96**(17): p. 1288-99.
42. Creecy, A., J.G. Damrath, and J.M. Wallace, *Control of Bone Matrix Properties by Osteocytes.* Front Endocrinol (Lausanne), 2020. **11**: p. 578477.
43. Wang, D., et al., *Multifunctional inorganic biomaterials: New weapons targeting osteosarcoma.* Front Mol Biosci, 2022. **9**: p. 1105540.
44. Zhang, Y., et al., *Progress in the chemotherapeutic treatment of osteosarcoma.* Oncol Lett, 2018. **16**(5): p. 6228-6237.
45. Ma, X., J. Zhao, and H. Feng, *Targeting iron metabolism in osteosarcoma.* Discov Oncol, 2023. **14**(1): p. 31.
46. Chen, Y., et al., *Advances in targeted therapy for osteosarcoma based on molecular classification.* Pharmacol Res, 2021. **169**: p. 105684.
47. Liu, J., et al., *Identification of Small-Molecule Inhibitors for Osteosarcoma Targeted Therapy: Synchronizing In Silico, In Vitro, and* In Vivo *Analyses.* Front Bioeng Biotechnol, 2022. **10**: p. 921107.
48. Shiravand, Y., et al., *Immune Checkpoint Inhibitors in Cancer Therapy.* Curr Oncol, 2022. **29**(5): p. 3044-3060.
49. Ritter, J. and S.S. Bielack, *Osteosarcoma.* Ann Oncol, 2010. **21 Suppl 7**: p. vii320-5.
50. de Azevedo, J.W.V., et al., *Biology and pathogenesis of human osteosarcoma.* Oncol Lett, 2020. **19**(2): p. 1099-1116.